

# Phase Formation Study of SnS Nanoparticles Synthesized Through PVP Assisted Polyol Method

**Benjamin Hudson Baby and D. Bharathi Mohan\***

Department of Physics, School of Physical, Chemical and Applied Sciences,

\*Corresponding author Email: \*d.bharathimohan@gmail.com

**Abstract.** The optimization study on the preparation of single phase of SnS nanoparticles by varying Sn:S source concentration ratio (1:1, 1:6 and 1:12M) through PVP assisted polyol synthesis method is successfully investigated. The single phase formation, crystal structure, surface morphology and optical properties of SnS nanoparticles have been studied using characterization techniques such as confocal Raman spectrometer, SEM, HR-TEM, UV-VIS-NIR spectrophotometer and spectrofluorometer. Confocal Raman as well as selected area electron diffraction analyses confirmed the single phase formation of SnS NPs with orthorhombic crystal structure at 1:12 ratio whereas SnS<sub>2</sub> and Sn<sub>2</sub>S<sub>3</sub> phases formed for lower sulphur concentration. Surface morphology reveals the formation of SnS nanorods predominantly, due to the addition of PVP which act as a capping agent. Band gap calculation from tauc plot showed direct band gap of 1.45 eV for single phase SnS with orthorhombic crystal structure, which can be used as an absorber layer in thin film solar cells. The observed shift in the band gap value is discussed in detail with the support of chemical structure analysis. The PL spectra of samples consists of 3 major peaks; the peak at 411 nm (3.03 eV) corresponds to Sn vacancy ( $V_{Sn}$ ), the peak at 435 nm (2.86 eV) corresponds to tin interstitial ( $I_{Sn}$ ) and peak at 459 nm (2.70 eV) corresponds to sulphur vacancy ( $V_S$ ). Whereas the additional peaks observed by decreasing the sulphur concentration to 0.6 and 0.1 M corresponds to the band edge emission of Sn<sub>2</sub>S<sub>3</sub> and SnS<sub>2</sub> respectively.

## 1. Introduction

Tin (II) sulphide is a suitable material to replace the absorber layer in thin film solar cells (TFSC) due to its excellent physical, optical and electrical properties which is equally good or still better than the existing absorber materials such as CdTe, CIGS, CZTS. SnS has a direct band gap value of 1.38 eV which is close to the optimum value of 1.5 eV for the efficient absorption of electromagnetic radiation in the visible region. It has very high absorption coefficient of  $10^{-5} \text{ cm}^{-1}$  compared to CdTe [1-3]. It exhibit P-type conductivity, its constituent elements are abundant in nature and these elements are less toxic and environmentally safe to handle. SnS exhibit orthorhombic crystal structure with lattice parameters  $a=0.4329\text{nm}$ ,  $b=1.1192\text{nm}$  and  $c=0.3984\text{nm}$  [JCPDS card no 39-0354]. In practice the highest efficiency achieved by SnS solar cell is only 4.4% [4]. This low efficiency may be due to the presence of impurity phases, grain boundaries and also due to the poor device fabrication techniques [5].

In this work, SnS nanoparticles (NPs) are prepared at a reaction temperature of 150 °C under open atmospheric conditions by using simple PVP assisted polyol synthesis method where ethylene glychol is the reaction medium which acts as the reducing agent and PVP is the capping agent which controls the agglomeration and ensures the monodispersity of NPs. It has already confirmed that the reaction



temperature and sulphur precursor plays a major role in controlling the surface morphology of SnS NPs [6]. Also it has reported that capping effect enhance the electrical properties of NPs by the rapid separation of electron –hole pair [7]. So here, by varying Sn:S source concentration ratio, optimized the formation of single phase of SnS with an optimum band gap value to use as an absorber layer in thin film solar cells.

## 2. Experimental Details

SnS NPs were prepared by using ethylene glycol (EG) (Qualigens fine Chemicals) as the reducing agent and polyvinylpyrrolidone (PVP) (Spectrochem Pvt. Ltd. Mumbai) as the capping agent to control the particle size of SnS. For the preparation of SnS high pure (reagent grade)  $\text{SnCl}_2$  and  $\text{Na}_2\text{S}$  salts used as the tin and sulphur precursors obtained from (Merck Specialties Pvt. Ltd, Mumbai.) and Finar (Finar Chemicals Ltd, Mumbai) respectively. Initially 0.1M of  $\text{SnCl}_2$ , 0.1M of  $\text{Na}_2\text{S}$  and 0.15M of PVP prepared in 10 ml of EG separately. Then add  $\text{Na}_2\text{S}$  and PVP simultaneously drop by drop into  $\text{SnCl}_2$  solution which was already placed in silicon oil bath at 150 °C and after the addition, the solution color changes to dark brown indicating the formation of SnS. Then solution was collected and quenched in a water bath after 20 minutes. This colloidal solution was washed several times using centrifuge at 5000rpm. Then, a thick (few microns) film of SnS was prepared by a simple drop casting technique. Following the above procedure, a set of experiment was carried out by changing Sn:S molarity ratio from 1:1 to 1:6 and 1:12 by fixing the PVP concentration at 0.15M.

The chemical structure of as deposited films was studied using confocal Raman spectrometer (ReinshawinVia Raman Microscope, UK) with an excitation wavelength of 785 nm using Ar<sup>+</sup> laser. The surface morphology of the film was studied by using Hitachi (Model: S-3400N) scanning electron microscope (SEM) and high resolution transmission electron microscope (HR-TEM) (JEOL/JEM 2100). The absorbance spectra of colloidal solution were studied using UV-Vis-NIR spectrophotometer (Shimadzu UV-3600 Plus) from the wavelength range of 300 to 1000 nm. The emission spectra was recorded with an excitation wavelength of 350 nm using spectrofluorometer (FLUOROLOG-FL3-11), equipped with Xenon lamp-450.

## 3. Results and Discussion

Raman spectroscopy is an efficient, sensitive and nondestructive technique to study the phase formation of different tin sulphide phases such as SnS,  $\text{SnS}_2$ ,  $\text{Sn}_2\text{S}_3$  with their distinct Raman shift. SnS has orthorhombic crystal structure and according to group theoretical predictions it has 21 optical phonon modes and 12 of them are Raman active which are  $4A_g$  (40,  $218 \pm 2$ ,  $192 \pm 2$ ,  $95 \pm 2$   $\text{cm}^{-1}$ ),  $2B_{1g}$  (70, 208  $\text{cm}^{-1}$ ),  $4B_{2g}$  (70,  $290 \pm 4$ , 160,  $85 \pm 2$   $\text{cm}^{-1}$ ) and  $2B_{3g}$  (49,  $164 \pm 2$   $\text{cm}^{-1}$ ). The appearance of different modes depends upon the incident and scattered direction of radiation and direction of electric polarization vector of incident and scattered photons [8,3]  $2H\text{-SnS}_2$  has rhombohedral crystal structure with 6 optical phonon modes and 3 of them are Raman active observing at  $A_{1g}$  (315  $\text{cm}^{-1}$ ) and  $E_g$  (140 and 205  $\text{cm}^{-1}$ ) [9]. For  $\text{Sn}_2\text{S}_3$ , orthorhombic crystal structure with 60 vibrational modes and predominant Raman peaks are observed at 52, 60, 111, 183, 233 and 307  $\text{cm}^{-1}$  [3,10]

Figure 1 shows the observed Raman spectra of samples by varying the Sn:S source concentration ratio using an excitation wavelength of 785 nm. Raman analysis confirmed the presence of secondary phases such as  $\text{SnS}_2$  (314.5  $\text{cm}^{-1}$ ) and  $\text{Sn}_2\text{S}_3$  (59  $\text{cm}^{-1}$ ) along with SnS phase for Sn:S ratio 1:1 molarity while by increasing to 1:6 molarity ratio, formation of  $\text{SnS}_2$  phase is completely suppressed and for 1:12 molarity ratio single phase of SnS is formed. SnS Raman active peaks at  $218 \pm 2$  and  $164 \pm 2$   $\text{cm}^{-1}$  correspond to the vibration of Sn atom against S and the peak at  $290 \pm 4$   $\text{cm}^{-1}$  corresponds to the compressive mode of the layers along c axis [8]. Raman peak at 315  $\text{cm}^{-1}$  corresponds to the symmetric interlayer mode of  $\text{SnS}_2$  [9].

Table 1 shows the observed Raman modes of SnS,  $\text{SnS}_2$  and  $\text{Sn}_2\text{S}_3$  phases obtained from as prepared samples which is compared with the standard single crystal data [3,8-10]. The RI (%) of different tin sulphide phases from Raman spectra as shown in Table 2 indicating a systematic decrease in the

formation of secondary phases such as  $\text{SnS}_2$  and  $\text{Sn}_2\text{S}_3$  by increasing the Sn:S source concentration ratio [3]

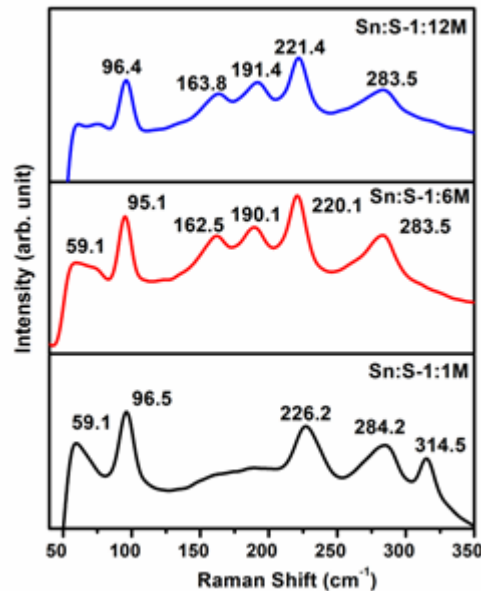


**Figure 1.** Raman spectra of samples prepared by varying Sn:S source concentration ratio 1:1 to 1:12 molarity using an excitation wavelength of 785 nm.

**Table 1.** Comparison of Raman modes of  $\text{SnS}$ ,  $\text{SnS}_2$  and  $\text{Sn}_2\text{S}_3$  obtained from as prepared samples compared with the standard single crystal data [3,8-10]

Single Crystal	SnS ( $\text{cm}^{-1}$ )					$\text{Sn}_2\text{S}_3$ ( $\text{cm}^{-1}$ )	$\text{SnS}_2$ ( $\text{cm}^{-1}$ )
	95±2	A <sub>g</sub> 218±2	192±2	B <sub>3g</sub> 164±2	B <sub>2g</sub> 290±4	60	A <sub>1g</sub> 315
Sn:S-1:1M	96.5	226.2	--	--	284.2	59.1	314.5
Sn:S-1:6M	95.1	220.1	190.1	162.5	283.5	59.1	--
Sn:S-1:12M	96.4	221.4	191.4	163.8	283.5	--	--

Figure 2 (a) shows SEM image of  $\text{SnS}$  NPs synthesized with Sn:S source concentration ratio of 1:12 molarity. Figure 2 (b) shows HR-TEM image confirming the predominant phase formation of  $\text{SnS}$  nanorods with 10-15 nm in width and 30-40 nm in length. The formation of single phase of  $\text{SnS}$  with orthorhombic crystal structure is confirmed by using selected area electron diffraction (SAED) pattern. Figure 2 (c) reveals the SAED pattern of  $\text{SnS}$  nanorods which is compared with the standard JCPDS card no 01-071-3679, again confirming pure  $\text{SnS}$  phase.

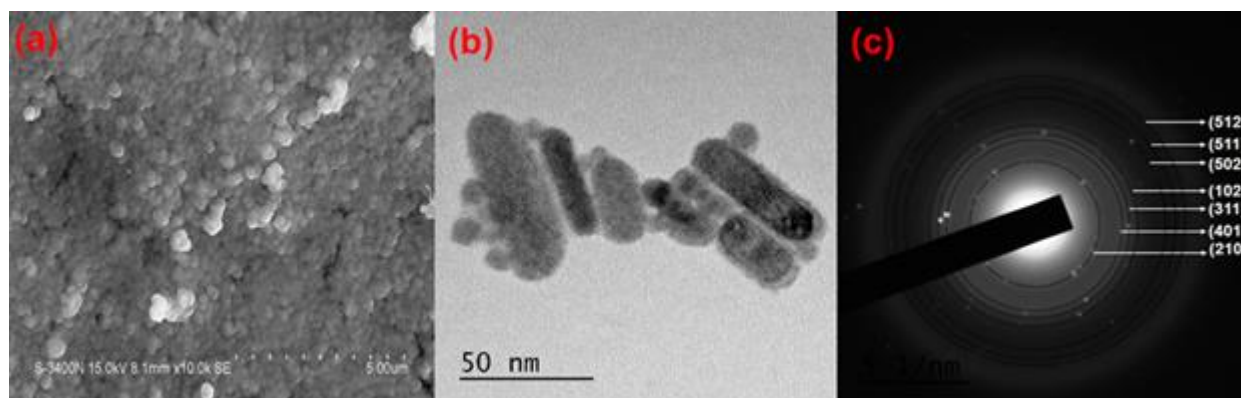


**Figure 2.** (a) SEM, 2 (b) HR-TEM images and 2 (c) SAED pattern of the sample with Sn:S molarity ratio 1:12.

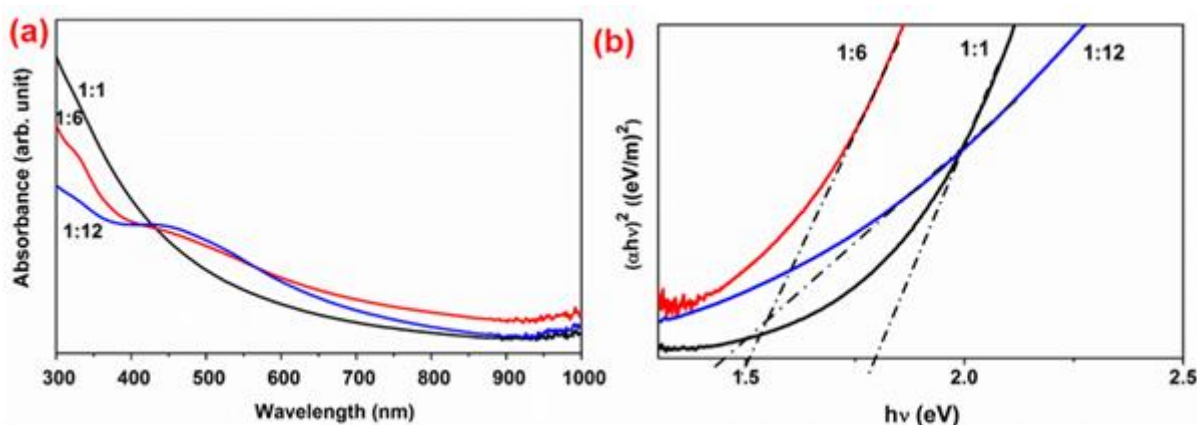


**Figure 3.** (a) Optical absorbance spectra and (b) tauc plot of samples with Sn:S source concentration ratio 1:1, 1:6 and 1:12 molarity

**Table 2.** Comparison of band gap value and relative intensity (RI) (%) (obtained from Raman analysis) of different Sn-S phases for the different Sn:S ratios.

Sn:S source concentration ratio (M)	Band gap (eV)	RI (%) of		
		SnS	SnS <sub>2</sub>	Sn <sub>2</sub> S <sub>3</sub>
1:1	1.79	37	31	32
1:6	1.5	64	0	36
1:12	1.45	100	0	0

Figure 3 (a) shows the absorbance spectra of samples dispersed in methanol in the wavelength range of 300 to 1000 nm. Figure 3 (b) shows the direct band gap calculation from x- intercept of tauc plot and the obtained values are shown in table 2 which is compared with the RI (%) of different tin sulphide phases calculated from Raman spectra. The observed shift in band gap value is due to the presence of secondary phases and also due the particle size effect. Initially, by increasing the concentration of S<sup>2-</sup> ions from 0.1M (1:1) to 0.6 M (1:6), the band gap is red shifted by 0.34 eV due to the complete

suppression of  $\text{SnS}_2$  phase in 1:6M, which has high band gap ( $E_g=2.3$  eV) value among entire tin sulphide phases [5]. Further increase in concentration of  $\text{S}^{2-}$  to 1.2 M results a red shift of 0.08 eV due to the formation of single phase of  $\text{SnS}$  ( $E_g=1.38$  eV) with complete suppression of  $\text{Sn}_2\text{S}_3$  phase ( $E_g=1.83$  eV) [5]. Sample with single phase of  $\text{SnS}$  shows a band gap value of 1.45 eV with a blue shift of 0.07 eV ( $E_g$ , bulk = 1.38 eV) due to the particle size effect [5]. Optical studies confirmed that the energy band gap of  $\text{SnS}$  is optimized to 1.45 eV which is matching with the band gap value of an absorber layer in thin film solar cells and it is obtained through controlling the formation of single phase of  $\text{SnS}$  by varying the concentration of  $\text{S}^{2-}$  ions.

Figure 4 (a) shows the PL spectra of  $\text{Sn-S}$  phase (synthesized by different  $\text{Sn:S}$  molarity ratios) with an excitation wavelength of 350 nm in the range 400 - 680 nm. It mainly consist of three peaks at 411, 435 and 459 nm. In addition to that, sample with  $\text{Sn:S}$  ratio 1:1M shows less intense peaks at 677, 614 and 571 nm, and for sample with ratio 1:6 M shows two peaks at 614 and 677 nm. The emission peak observed at 411 nm (3.03 eV) corresponds to tin vacancy ( $V_{\text{Sn}}$ ) which is responsible for its p type behaviour [11]. The peak at 435 nm (2.86 eV) corresponds to tin interstitial ( $I_{\text{Sn}}$ ) and peak at 459 nm (2.70 eV) corresponds to the sulphur vacancy ( $V_{\text{S}}$ ) [11] (Fig.4 (b)). The presence of high intense  $I_{\text{Sn}}$  defect with less intense  $V_{\text{S}}$  indicate the formation of  $\text{Sn}$  rich  $\text{SnS}$  phase for sample with  $\text{Sn:S}$  ratio 1:12M. Raman analysis confirmed the formation of single phase of  $\text{SnS}$  for  $\text{Sn:S}$ -1:12M and while by decreasing  $\text{S}^{2-}$  ion concentration secondary phases such as  $\text{SnS}_2$  and  $\text{Sn}_2\text{S}_3$  are also observed which is once again verified from PL analysis. For 1:6M, two additional peaks observed at 677 nm (1.83 eV) and 614 nm (2.01 eV) corresponds to the band edge emission and  $V_{\text{S}}$  of  $\text{Sn}_2\text{S}_3$  as shown in Fig.4 (b). It is already reported that the direct band gap of  $\text{Sn}_2\text{S}_3$  is various from 0.96 eV to 2 eV depends due to the quantum confinement effect. The third additional peak at 571 nm (2.17 eV) for 1:1M corresponds to the band edge emission of  $\text{SnS}_2$  where the band gap of  $\text{SnS}_2$  is 2.3 eV [5]. The observation of broad fluorescence emission spectra with many side emission bands for sample with  $\text{Sn:S}$  ratio 1:1M and 1:6M indicating enormous delay in recombination rate due to the presence of several shallow trap states or intrinsic near-band edge states slightly below the conduction band involving phonon-exciton and phonon-phonon interactions [12].

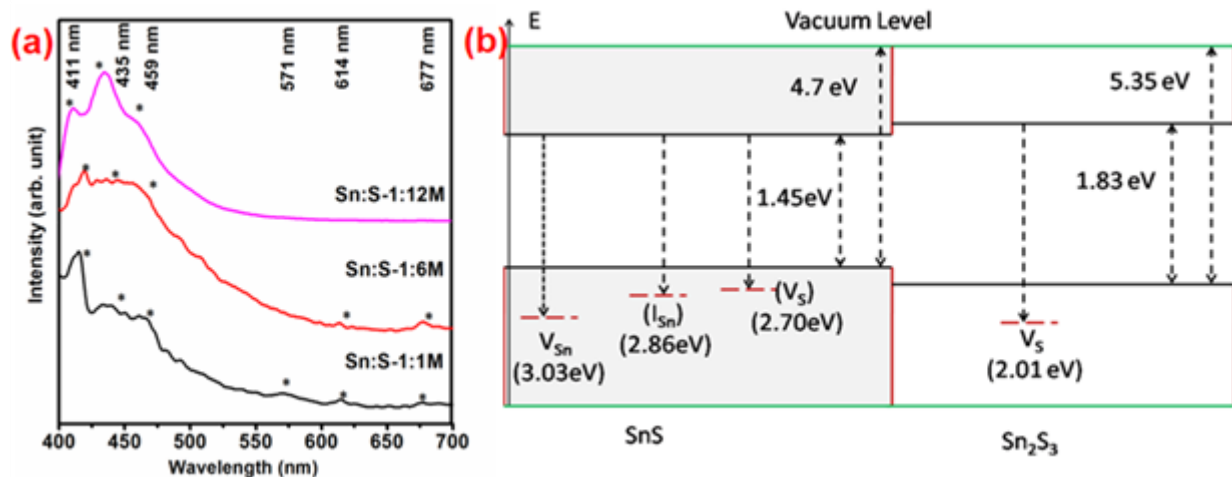


**Figure 4.** (a) Room temperature PL spectra of  $\text{Sn-S}$  samples prepared with 1:1, 1:6 and 1:12 molar ratios. (b) Schematic band diagram for the point defects formed in  $\text{SnS}$ - $\text{Sn}_2\text{S}_3$  systems.  $V_{\text{S}}$ – sulfur vacancy,  $V_{\text{Sn}}$ – tin vacancy,  $I_{\text{Sn}}$ – tin interstitial. The energy levels are drawn from the analysis of absorption and emission spectra.



#### 4. Conclusion

In conclusion, single phase of SnS nanoparticles were successfully synthesized using PVP assisted polyol method for the reaction temperature of 150 °C by varying Sn:S source concentration ratio as 1:1, 1:6 and 1:12M. Chemical structural analysis confirmed the formation of SnS<sub>2</sub> and Sn<sub>2</sub>S<sub>3</sub> as the secondary phases for lower sulphur source concentration. While the formation of single phase of SnS nanoparticles with orthorhombic crystal structure was confirmed with source concentration ratio of 1:12M as evident from chemical as well as crystal structural analysis. HR-TEM analysis confirmed the formation of SnS nano rods with an aspect ratio of 0.375. The observed red shift in the band gap value by increasing the source concentration ratio is due to the formation of secondary phases as observed from chemical structural analysis. Single phase of SnS shows a band gap value of 1.45 eV which can be used as an absorber layer in thin film solar cells. Photoluminescence analysis further confirmed the formation of single phase of SnS for 1:12M source concentration ratio and the proposed band diagram shows the presence of three intrinsic defects such as tin interstitial (I<sub>Sn</sub>), tin vacancy (V<sub>Sn</sub>) and sulphur vacancy (V<sub>S</sub>).

#### 5. Acknowledgments

The work is supported by University Grant Commission (UGC) - Major Project (F. No 4151868/2012 (Sr)). BHB sincerely UGC-BSR for providing Research Fellowship.

#### 6. References

- [1] Y. Hirai, Y. Kurokawa, and Akira, Jpn.J. Appl. Phys. Sci. 53, 012301 (2013).
- [2] M. A Green, K. Emery, Y. Hishikawa, W. Warta and E. D. Dunlop, Prog. Photovoltaics 23, 1–9 (2015).
- [3] B. H. Baby and D. B. Mohan, AIP Conf. Proc. 1665, 050171 1 (2015).
- [4] P. Sinsermsuksakul, L. Sun and S. W. Lee, Advanced Energy Materials DOI :10.1002/aenm.201400496 (2014).
- [5] L. A. Burton, D. Colombara, R. D. Abellon, F. C. Grozema, L. M Peter, T. J. Sevenije and G. Dennler, Chem. Mater. 25, 4908 (2013).
- [6] Z. Niu and Y. Li, Chem. Mater. 26, 72 (2014).
- [7] S. Jana, N. Mukherjee, B. Chakraborty, B. C. Mitra and A. Mondal, Appl. Surf. Sci. 300, 154 (2014).
- [8] H. R. Chandrasekhar, R. G. Humphreys, U. Zwick and M. Cardona, Phys. Rev. B 15, 2177 (1977).
- [9] A.J. Smith, P. E. Meek and W. Y. Liang, J. Phys. C: Solid State Phys.10, 1321 (1977).
- [10] H. R. Chandrasekhar and D. G. Mead, Phys. Rev. B 19, 932 (1979).
- [11] M. Devika, N. K. Reddy, M. Prashantha, K. Ramesh, S. V. Reddy, Y. B. Hahn and K. R. Gunasekhar, Phys. Status Solidi A 207, 1864 (2010).
- [12] D. B. Mohan, V. S. Reddy and C. S. Sunandana, Appl. Phys. A 86, 73 (2007).